NAVAL POSTGRADUATE SCHOOL
Monterey, California

THESIS

AN EXPERIMENTAL STUDY OF HIGH HEAT FLUX REMOVAL USING MICRO-DROPLET SPRAY COOLING

by

Matthew A Cryer

June 2003

Thesis Advisor: Ashok Gopinath

Approved for public release; distribution is unlimited.

THIS PAGE INTENTIONALLY LEFT BLANK

REPORT DOCUMENTATION PAGE			Form Approved OMB No. 0704-0188
Public reporting burden for this collection of information is estimated to average 1 hour per response, including the time for reviewing instruction, searching existing data sources, gathering and maintaining the data needed, and completing and reviewing the collection of information. Send comments regarding this burden estimate or any other aspect of this collection of information, including suggestions for reducing this burden, to Washington headquarters Services, Directorate for Information Operations and Reports, 1215 Jefferson Davis Highway, Suite 1204, Arlington, VA 22202-4302, and to the Office of Management and Budget, Paperwork Reduction Project (0704-0188) Washington DC 20503.			
1. AGENCY USE ONLY *(Leave blank)*	**2. REPORT DATE** June 2003	**3. REPORT TYPE AND DATES COVERED** Master's Thesis	
4. TITLE AND SUBTITLE: An Experimental Study of High Heat Flux Removal Using Micro-Droplet Spray Cooling			**5. FUNDING NUMBERS**
6. AUTHOR(S) Matthew A. Cryer			
7. PERFORMING ORGANIZATION NAME(S) AND ADDRESS(ES) Naval Postgraduate School Monterey, CA 93943-5000			**8. PERFORMING ORGANIZATION REPORT NUMBER**
9. SPONSORING /MONITORING AGENCY NAME(S) AND ADDRESS(ES) N/A			**10. SPONSORING/MONITORING AGENCY REPORT NUMBER**
11. SUPPLEMENTARY NOTES The views expressed in this thesis are those of the author and do not reflect the official policy or position of the Department of Defense or the U.S. Government.			
12a. DISTRIBUTION / AVAILABILITY STATEMENT Approved for public release; distribution is unlimited.			**12b. DISTRIBUTION CODE**

13. ABSTRACT ***(maximum 200 words)***

Recent studies have shown that thermophotovoltaic (TPV) technology is a promising source of high power density generation. Enhanced TPV systems can theoretically provide power densities of up to 100 W/cm^2. The inherent ineffiencies in the system dictate that up to 90% of that energy is not converted to electrical power, and must be removed as waste heat to ensure that the components are maintained at a reasonable operating temperature. The present study addresses this issue by investigating the suitability of using spray cooling techniques to remove heat generated by power densities of up to 100 W/cm^2. A simple, scaleable experiment was designed using low-cost commercially available components to study the effects that spray mass flux and droplet size have on the heat removal capacity of the system. A series of nozzles were used so that mass flux and droplet size could be studied independently, giving high resolution to the data so that predictive correlations could be developed over the range of parameters varied in the study.

14. SUBJECT TERMS Spray Cooling, High Heat Flux, Nucleate Boiling, Heat Transfer Enhancement			**15. NUMBER OF PAGES** 61
			16. PRICE CODE
17. SECURITY CLASSIFICATION OF REPORT Unclassified	**18. SECURITY CLASSIFICATION OF THIS PAGE** Unclassified	**19. SECURITY CLASSIFICATION OF ABSTRACT** Unclassified	**20. LIMITATION OF ABSTRACT** UL

NSN 7540-01-280-5500 Standard Form 298 (Rev. 2-89)
Prescribed by ANSI Std. 239-18

THIS PAGE INTENTIONALLY LEFT BLANK

Approved for public release; distribution is unlimited.

AN EXPERIMENTAL STUDY OF HIGH HEAT FLUX REMOVAL USING MICRO-DROPLET SPRAY COOLING

Matthew A. Cryer
Lieutenant, United States Naval Reserve
BSME, University of New Mexico, 1998

Submitted in partial fulfillment of the
requirements for the degree of

MASTER OF SCIENCE IN MECHANICAL ENGINEERING

from the

NAVAL POSTGRADUATE SCHOOL
June 2003

Author: Matthew A Cryer

Approved by: Ashok Gopinath
Thesis Advisor

Young W. Kwon
Chairman, Department of Mechanical Engineering

THIS PAGE INTENTIONALLY LEFT BLANK

ABSTRACT

Recent studies have shown that thermophotovoltaic (TPV) technology is a promising source of high power density generation. Enhanced TPV systems can theoretically provide power densities of up to 100 W/cm^2. The inherent ineffiencies in the system dictate that up to 90% of that energy is not converted to electrical power, and must be removed as waste heat to ensure that the components are maintained at a reasonable operating temperature. The present study addresses this issue by investigating the suitability of using spray cooling techniques to remove heat generated by power densities of up to 100 W/cm^2. A simple, scaleable experiment was designed using low-cost commercially available components to study the effects that spray mass flux and droplet size have on the heat removal capacity of the system. A series of nozzles were used so that mass flux and droplet size could be studied independently, giving high resolution to the data so that predictive correlations could be developed over the range of parameters varied in the study.

THIS PAGE INTENTIONALLY LEFT BLANK

TABLE OF CONTENTS

LIST OF FIGURES

THIS PAGE INTENTIONALLY LEFT BLANK

LIST OF TABLES

THIS PAGE INTENTIONALLY LEFT BLANK

ACKNOWLEDGMENTS

I would like to thank Professor Ashok Gopinath for his superior insight and steady support throughout this research. I also thank my wife for her unwavering support, without which this project would not have been possible.

THIS PAGE INTENTIONALLY LEFT BLANK

LIST OF SYMBOLS

q''	Heat flux, W/cm^2
D_{32}	Sauter Mean Diameter, droplet size, μm
k	thermal conductivity, W/m-K
$\dot{V}$	volumetric flowrate, mL/s
g	gravitational acceleration, m/s^2
h_{fg}	latent heat of vaporization, kJ/kg
c_{pl}	specific heat of fluid in liquid phase, kJ/kg-K
c_{pv}	specific heat of fluid in vapor phase, kJ/kg-K
$q''_{s,R}$	heat flux predicted by Rohsenow correlation
ρ_l , ρ_v	density of fluid in liquid and vapor phases, respectively, kg/m^3
μ	viscosity of fluid, N-s/m^2
σ	surface tension of fluid, N/m
ΔT_e	excess temperature, or temperature of surface minus saturation temperature of fluid
A_{flux}	Area flux of fluid, cm^2/s

THIS PAGE INTENTIONALLY LEFT BLANK

I. INTRODUCTION

There has recently been a renewed interest in the study and development of thermophotovoltaic (TPV) technology for the purpose of power generation. This technology provides an elegant form of energy conversion in that it has fewer moving parts, fewer components, and a simpler overall design. Recent work has shown the potential for very high power density (on the order of 100 W/cm^2) generation using Micro-TPV (MTPV) systems. The different subsystems of this new technology, however, must also be carefully designed and proven before the technology as a whole can become a viable option for high power generation, such as in the nuclear power industry.

A typical MTPV system consists of a heat source, an emitter that transfers the energy of the heat source by radiation at a known wavelength, a semiconductor receiver at very close (sub-micron) spacing to the emitter which converts the thermal photonic energy to electrical current, and an electrical power distribution system. The inherent inefficiencies in the energy conversion process means that a large fraction of the radiated energy from the emitter is dissipated as waste heat in the receiver that needs to be removed to maintain it at its operating temperature. The present study concerns itself with this very issue.

High heat flux removal techniques have become the subject of many recent studies due to its importance in several modern industrial and technological applications, such as in cooling of electronic components, in nuclear power generation, and laser applications (Ortiz [1999]). The waste heat generated by an MTPV system could potentially be on the order of 10-100 W/cm^2 and can only be realistically removed through phase change heat transfer processes. Phase change heat transfer is characterized by very high heat flux for low temperature differentials between the hot surface and the heat transfer fluid.

Some of the phase change heat removal techniques under recent study are convective flow boiling in micro-channels (Kearns [2002]), jet-impingement cooling (Xia [2002], spray cooling (Ortiz [1999], Xia [2002]), and mist cooling (Liu [2002]). Although convective flow boiling techniques offer high heat transfer rates, they cannot match the larger heat removal rates that are achieved in spray cooling due to the extent of directness of contact between the liquid and the surface, as well as the large contact area itself that is present for a given liquid volume. Jet-impingement cooling also provides high heat flux removal capacity; it is, however, a very localized effect within the impingement zone and can lead to separation of the liquid layer from the surface during vigorous boiling, leading to dryout and hotspots, which can result in catastrophic failure of temperature-sensitive equipment. Typical results of phase change cooling schemes are summarized in Table 1.

Cooling Type	**CHF (W/cm^2)**	**ΔT (Wall-liquid)**
Spray Cooling	600	Small
Jet Boiling on micro-surface	500	Large
Jet Boiling on macro-surface	100-300	Large
Subcooling Convective Boiling	500	Large
Mini-Channel Convective Boiling	200	Large
Micro-Channel Convective Boiling	300	Large
Pool Boiling	100	Large
Heat Pipe	10-30	Large

Table 1. Critical Heat Flux and Temperature Rise in Phase-Change Cooling Schemes

Spray and mist cooling techniques, on the other hand, provide a liquid stream that is broken into a large number of tiny (mean diameters range from 1-100 microns) droplets that completely blanket the heated surface and provide spatial uniformity in the heat removal process, at the same time providing a quasi-stable liquid film on the surface at all times. Sprays are classified as pressure or atomized based on the method used for liquid breakup. Pressure sprays are formed by supplying the liquid at high pressure through the small orifices of a nozzle. Atomized sprays or mists are generated by the presence of a co-existent high-pressure gas stream that breaks up the liquid into "atomized" droplets. This technique is commonly referred to in the literature as air-assisted spray. Although mists provide a potentially better cooling performance due to their smaller droplet size, there are practical difficulties associated with the presence of the gas stream in the phase change process that now becomes an undesirable non-condensable species. This can be especially problematic in a closed-loop scheme or schemes that involve the phase change taking place in a partial vacuum.

The present study is an investigation of the pressurized spray technique using commercially available nozzles and liquid delivery systems. Its goal was to provide an understanding of the suitability of using spray cooling to remove the potential waste heat generated by an MTPV system by using a simple, scaleable experimental model under a variety of flow rates, droplet sizes, and surface temperatures.

A. PREVIOUS WORK

There are several references in the literature that have investigated spray cooling as a high heat flux removal technique. The effects that the mass flow rate (Halvorson [1994], Webb [1992], Xia [2002], Yao [1987]), the impact angle (Ortiz [1999], McGinnis [1969]), the surface roughness (Ortiz [1999], Pais [1992], Bernardin [1997]), and reduced gravity (Kato [1994], Qiao [1996]) may have on the heat removal capacity have been conducted under transient conditions. An extensive experiment conducted by Ortiz, et al, [1999] investigated the effects of mass flow, impact angle, surface roughness, and degree of sub cooling under steady state conditions. They concluded that both the steady state

and transient conditions show similar boiling behavior with very good data overlap and that data found under transient conditions may be valid for steady-state conditions. A comparison between the present study and previous work is given in Table 2.

Author	Droplet Diameter	Water Temperature, C	Nozzle Type	Mass flow rate, L/h
Halvorson et al [1994]	2.96-3.41 mm	20	19 gauge needle	0.07
Yang et al. [1993]	10-18 μm	20	Air assisted	0.5
Gaugler [1966]	128-150 μm	20	Full cone	0.86
Ortiz et al. [1999]	85-100 μm	24	Full cone	1.48-1.89
Kato et al. [1994]	110 μm	20	Full cone	2.04
Toda [1971]	88-146 μm	55-100	Air assisted	2.92
Cryer [2003]	19-32 μm	20	Full cone	1.96-9.66

Table 2. Comparison between the present study and previous works

The present study departs from previous works in that it studies a much wider range of mass flow rates and droplet sizes independently, giving much finer resolution to the data so that better correlations might be developed to predict the capacity of the system. The droplet sizes studied presently are at the low limit of commercially available full-cone pressurized spray nozzles and approach the sizes achieved by air-assisted mist cooling schemes.

II. EXPERIMENTAL SETUP

A. SPRAY DELIVERY SYSTEM

The spray system is illustrated schematically in Figure 1 and displayed in Figure 2. It consists of a pressurized Nitrogen cylinder connected via regulator to the liquid pressure vessel. The fluid was delivered to the nozzle through ¼ -inch stainless steel tubing, which was instrumented with a micro-flow meter, a pressure gage, and an inline type E thermocouple probe.

The nozzles utilized were Hago B-Type full-cone nozzles with a 70 degree cone angle. The droplet sizes were in the range 18-35 μm, as reported by the manufacturer, and flow rates varied from 1.96 to 26.76 L/hr, as reported by the manufacturer and verified during system testing and calibration. A typical nozzle is shown in Figure 3. Distilled water was used as the spray medium in all cases to ensure that there were no impurities, particulate or ionic, which could have an unpredictable effect on the heat transfer or hydraulic properties of the system.

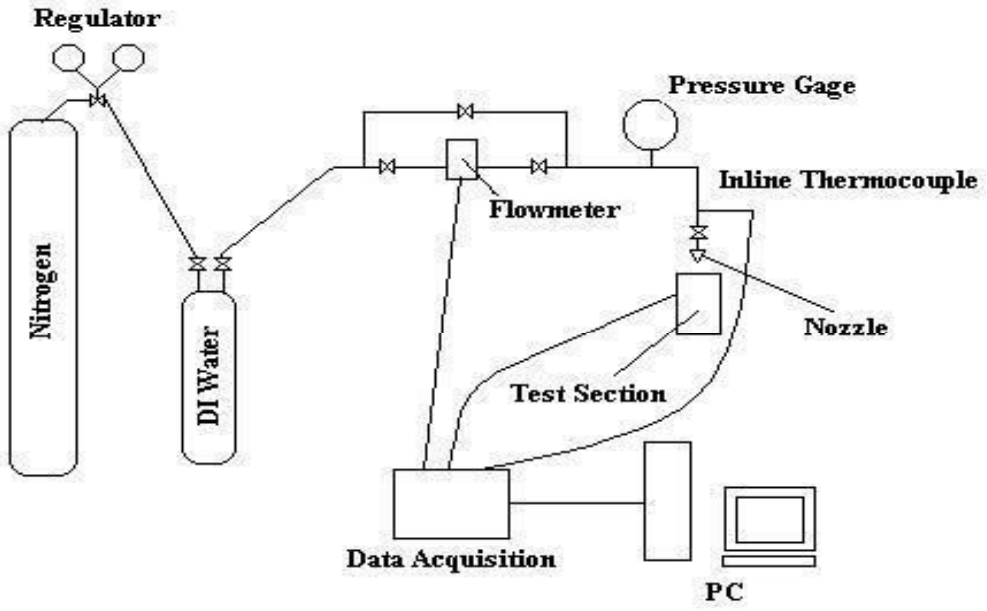

Figure 1. Spray Delivery System Schematic

Figure 2. Spray System

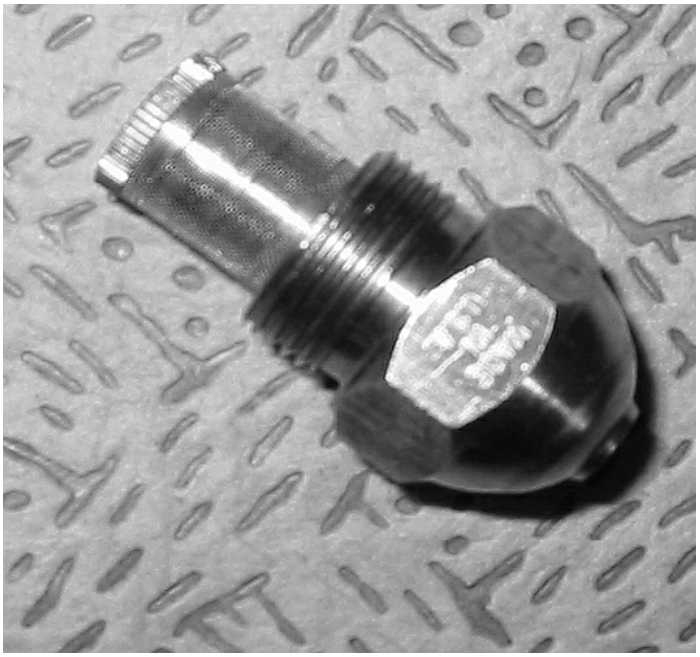

Figure 3. Typical Nozzle

B. TEST SECTION

The main components of the test section are the heater block and the instrumented specimen. These components are illustrated schematically in Figure 4 and photographically in Figures 5 and 6. The assembled test section is shown in Figure 7. The heater block was a 2.8 inch diameter by 3.5 inch long copper cylinder, in which was embedded 4 Watlow 1000 Watt (nominal) cartridge heaters. The resistance of each heater was measured and the heaters were wired in a series-parallel configuration to provide a 13.02Ω equivalent resistance. The heaters were powered from a Staco variable transformer that provided a continuously variable voltage source from 0 to 237 Volts. The heater block was placed in a 4-inch diameter PVC tube, and the block was insulated on all sides except the top. This was done to ensure largely one-dimensional heat transfer with minimal losses from the sides. The block was instrumented with three type E thermocouple probes spaced at 3.175 mm so that the heat flux could be determined.

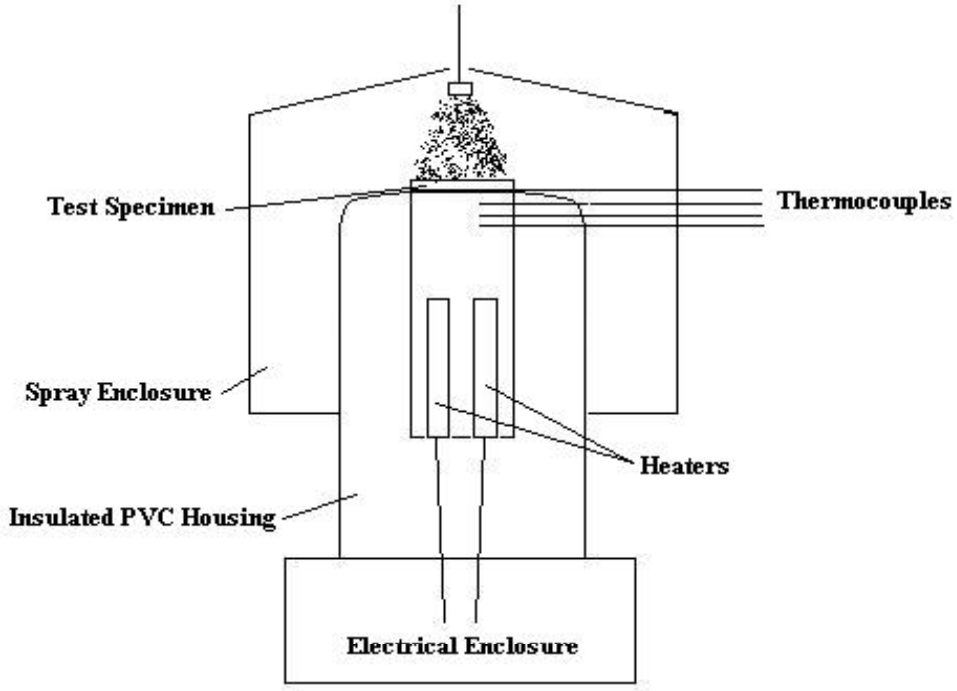

Figure 4. Schematic of Test Section

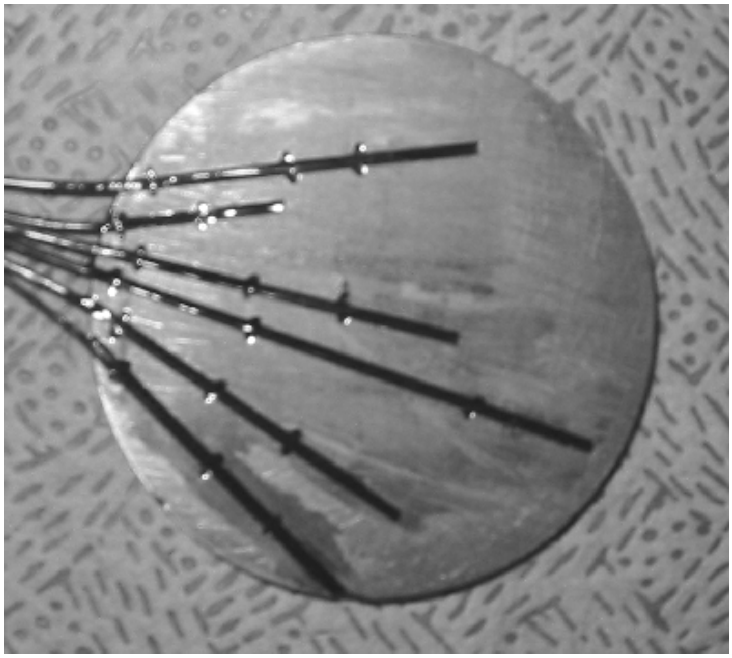

Figure 5. View of thermocouple placement on underside of test specimen

Figure 6. Underside view of heater block with embedded heaters and thermocouples

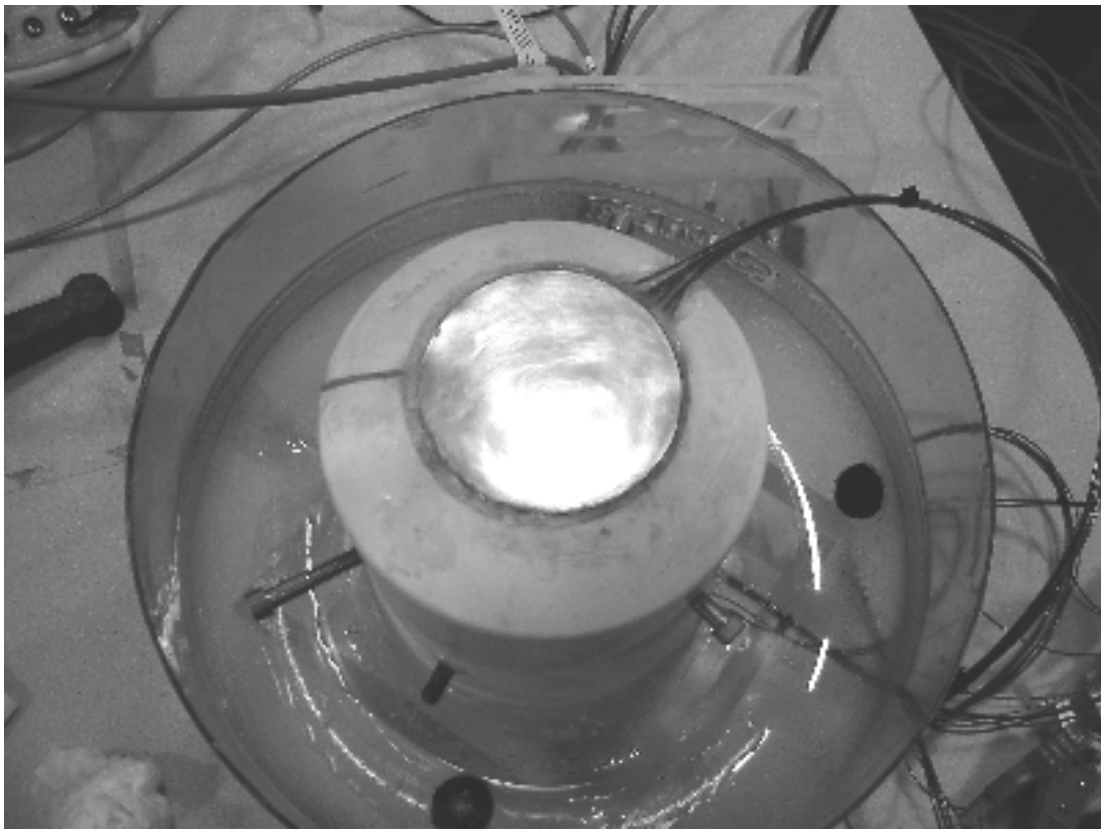

Figure 7. Assembled Test Section

Thermocouples were also placed on the side of the block and at the inner diameter of the PVC enclosure so that heat losses could be characterized by the temperature gradient across the insulation. The test specimen was a thin copper disk of 2.8 inch diameter instrumented with six type E thermocouples placed such that adequate radial and angular coverage was given to verify isothermal surface temperatures, as shown in Figure 3. The total power capacity of the heaters of 4,314 Watts combined with the surface area of the disk at 40 cm^2 provided a peak power density of 107.9 W/cm^2.

C. INSTRUMENTATION AND DATA ACQUISITION

The output of all thermocouples and the pressure gage were connected to an HP 3852 data acquisition unit, which was in turn connected to a PC running LabView software. The fluid temperature was measured using a type E thermocouple probe placed as close to the nozzle as possible. The heater block was instrumented with three type E thermocouples placed at 0.3175 cm intervals vertically so that the one-dimensional heat flux in the axial direction could be calculated. These were placed in the block using thermal epoxy to eliminate air gaps. The surface temperature of the test specimen was determined using six type E thermocouples, placed in the locations shown in Figure 5. These were affixed using the same thermal epoxy, as close to the wetted surface as possible. A thermocouple was affixed to the side of the heater block with the thermal epoxy and another was placed on the inner radius of the PVC enclosure at the same vertical placement to facilitate the determination of energy losses.

III. EXPERIMENTAL PROCEDURE

A. CALIBRATION AND UNCERTAINTY ANALYSIS

The main variables observed during the experiment were the temperatures of the heated element and the mass flow rate of the spray. The flow rate of the spray was determined through extensive testing of the system. Each nozzle was sprayed at the pressure setpoints used for the present experiment and a stopwatch was used to measure the amount of time it took to fill 20 mL in a graduated cylinder. The cylinder was graduated in 1 mL increments, giving +/- 0.5 mL accuracy, and the stopwatch timing was accurate to within 0.1 seconds. This gives a determination of the flow rate to within +/- 5% at the highest flows, with greater accuracies at the lowest flows. Several independent tests were done at each setpoint with a high degree of repeatability. A typical flow versus pressure calibration curve is provided in Appendix C.

The heat flux was calculated using the temperature gradient provided by the three levels of thermocouples in the heater block assuming one-dimensional heat transfer and Fourier's Law:

$$q'' = k\frac{\Delta T}{\Delta x} \tag{1}$$

where k is the thermal conductivity of the copper (392.9 W/m/C), ΔT is the temperature difference between the thermocouples, and Δx is the distance between the thermocouples. The uncertainty in the heat flux was calculated to be

$$\frac{\varepsilon_q}{q} = \sqrt{\left(\frac{\varepsilon_x}{\Delta x}\right)^2 + \left(\frac{\varepsilon_T}{\Delta T}\right)^2} \tag{2}$$

where ε_x and ε_T are the uncertainty in the distance measured and in the temperature reading, respectively. The thermocouple error was taken to be +/- 0.5 ^{o}C and the uncertainty in the distance between the thermocouples was +/- 0.00005 mm. These values provide a total uncertainty in the heat flux of 6.4% at a heat flux of 100 W/cm^2.

The resistance of each of the of the cartridge heaters was measured and the output of the variable transformer was instrumented with a multi-meter so that the total power input could be calculated as follows

$$P = \frac{V^2}{R_{eq}} \tag{3}$$

This allowed a "sanity check" on the heat flux calculations, as the heat flux calculated by the thermal gradient in the heater block should be somewhat less than or equal to the input power.

The thermal gradients observed across the insulation indicated minor radial energy losses as compared to the heat flux in the axial direction, and were considered negligible for the present experiment. Additionally, it allowed for the assumption that the heat flux was mainly one-dimensional in the axial direction.

No independent tests were performed to verify manufacturer claims for the droplet sizes. According to the manufacturer, the droplet sizes are given as Souter Mean Diameter using a MUNHALL PSA–32 particle size analyzer which measures drops based on Fraunhofer's Diffraction Principle. These tests were verified by the manufacturer using a photomask test reticle which contains a known distribution of droplets per ASTM draft photomask / reticle method

B. PROCEDURE

The procedures developed for the present study were a result of the parameters under consideration and the response of the experimental apparatus during testing and calibration. Two variables were studied independently: mass flow rate and droplet size. The mass flow rates were determined during system calibration as previously described and the droplet sizes were as given by the manufacturer. The mass flow was controlled by throttling the flow to known pressure setpoints for each nozzle, while the droplet size was given by a nozzle/pressure lookup table. Droplet sizes at pressures not given by the manufacturer were determined by using a logarithmic extrapolation from the given points. A typical result of the line fit for the droplet size versus pressure is given in Figure 8.

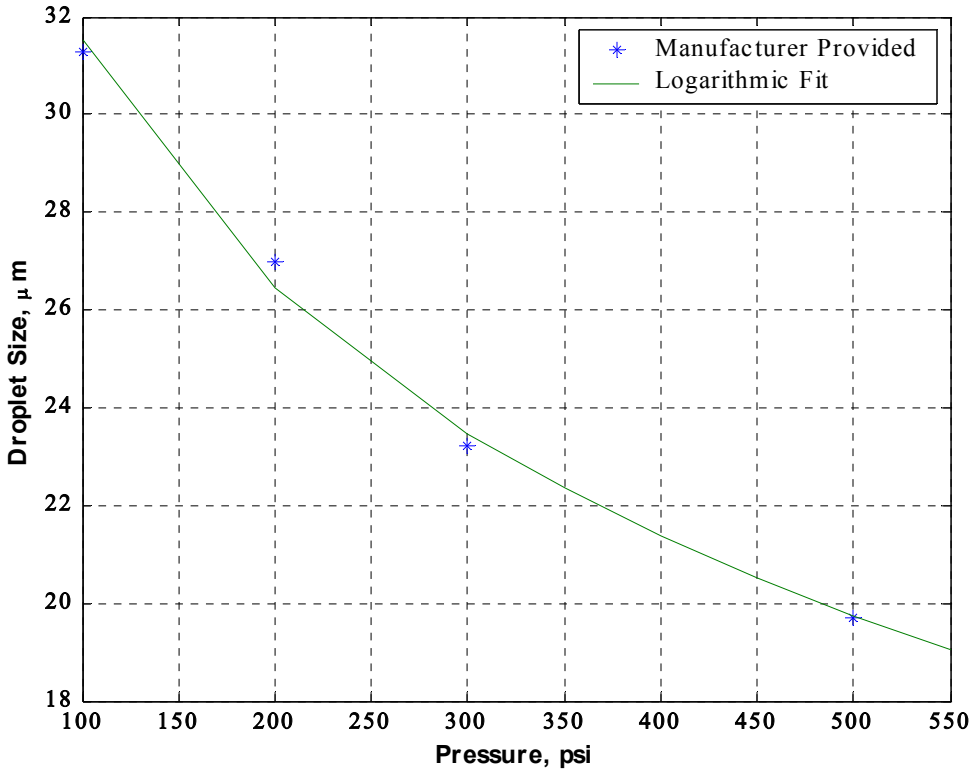

Figure 8. Line Fit for Droplet Size versus Pressure

Pressure	100 psi	200 psi	300 psi	350 psi	400 psi	450 psi	500 psi
Droplet Size	32 μm	26 μm	23 μm	22 μm	21 μm	20 μm	19 μm
Nozzle	**Flow Rates (mL/min)**						
B37	34.1	49.3	58.7	63.4	71	75.2	80.1
B50	45.8	63.2	78.1	90.1	93.5	101.4	113.4
B75	68.4	98.4	114.1	122.9	126.8	137.9	153.4
B100	93	132.5	161.3				

Table 3. Set of Experiments Performed

The experimental matrix for the pressure/flow/droplet size variation is exhibited in Table 3. Each nozzle/pressure combination sets the droplet size and the flow rate. Experiments were performed at each point in the table to determine the heat flux removed and the surface temperature of the disk, for a total of 24 sets of data. The surface of the test section was polished progressively with 600 and then 1000 grit grinding paper and then cleaned with alcohol to remove any oxidation and maintain a consistent "rough" surface before each experiment. The test section was leveled and the spray nozzle was aligned to maintain a 90-degree spray angle and to ensure an even spray distribution across the disk. The spray medium was taken at ambient temperature, and remained at an essentially constant 28 ^{o}C throughout the set of experiments.

The nozzle under consideration was installed in the system and the pressure at the Nitrogen regulator was set to 550 psi. The system was then lined up such that spray initiation could be accomplished by the turn of a single ball valve. After the spray system lineup was verified, a low voltage was applied to the heaters through the variable transformer to bring the heater block slowly up to temperature. Spray flow was initiated and the pressure set to 100 psi when the test section temperatures approached 85 ^{o}C. The voltage was then slowly increased at 2 to 5 Volt increments until the disk temperature reached a peak steady state temperature of approximately 105 ^{o}C. Steady state was defined to be when temperatures on the surface did not change over a period of three minutes. At this point, the data were recorded and the pressure was raised to the next setpoint, increasing the flow rate. The voltage was then increased as before until the surface temperature was brought back up to approximately 105 ^{o}C. This procedure was then repeated at each setpoint for the installed nozzle, then the test section was cooled to well below 100 ^{o}C at the high flow rate with the heaters de-energized before spray was stopped and the next nozzle installed. The procedure was then repeated for each nozzle in the series.

The surface temperature setpoint of 105 ^{o}C was chosen to ensure adequate excess temperature (T_{ex}) above the saturation point to produce nucleate boiling on the surface, yet be low enough to provide a margin of safety from critical heat flux (CHF), which could destroy the component being cooled. Although this point is not at the absolute

peak heat removal capacity of the system, it is more realistic in terms taking advantage of two-phase cooling yet maintaining a reasonable component temperature.

The heat flux of the system was calculated by taking the temperature gradient across the three thermocouples in the heater block and multiplying that by the thermal conductivity of pure copper (k), or

$$q'' = k\frac{\Delta T}{\Delta x}$$

where ΔT was taken as the average temperature difference between the two levels of thermocouples

$$\Delta T = \frac{(T_1 - T_2) + (T_2 - T_3)}{2}$$

where T_i is the thermocouple temperature at level i.

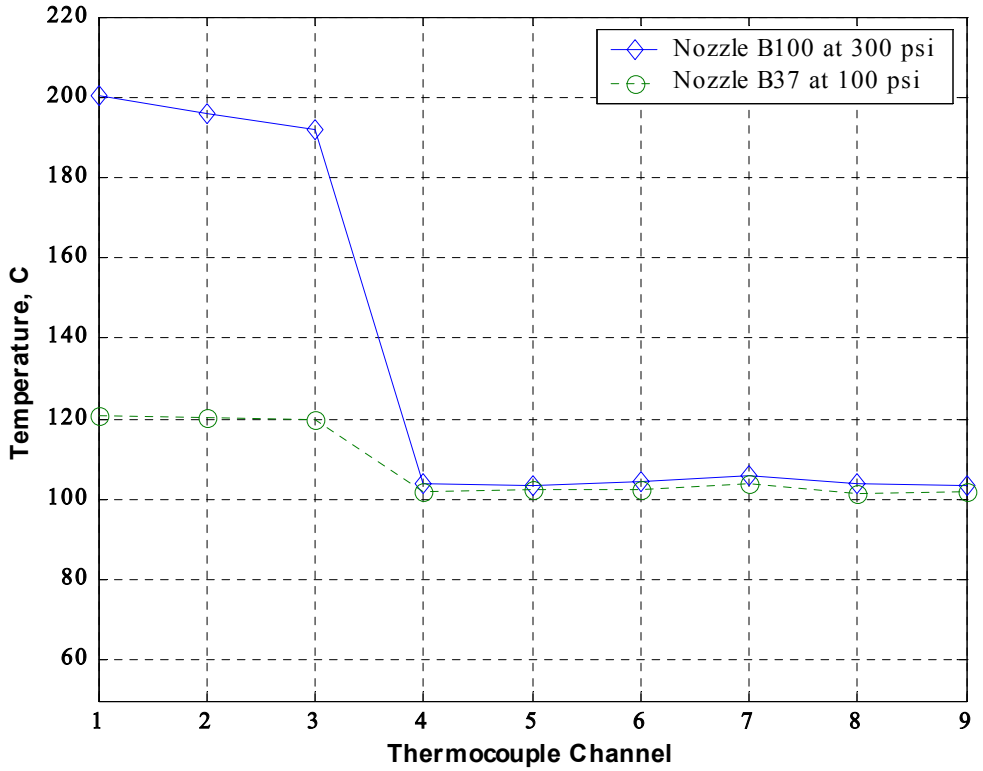

Figure 9. Experimental Temperature Profile in the heater block and test specimen for Nozzle B100 at 300 psi and Nozzle B37 at 100 psi

Typical experimental profiles for the temperature distribution in the heater block and across the test specimen are given in Figure 9. Channels 1-3 are the heater block thermocouples and channels 4-9 are the thermocouples arranged radially across the test specimen. The fairly flat temperature profiles in all cases suggest that the assumption of one-dimensional conduction axially through the test section to the surface was reasonable. It was observed during the experiments that the distribution across the test specimen took a flatter profile at the spray flow rate was increased. The large temperature gradient between the heater block and disk was due to the contact resistance between the heater block and the disk, and grew as higher voltages were applied. A thermal compound such as that used between computer CPU's and heat sinks was used to minimize that gradient as much as possible.

IV. RESULTS AND DISCUSSION

The experimental matrix allowed the data to be recorded in a fairly orderly manner and then processed such that the effects of droplet size for a given flow rate and the effects of flow rate for a given droplet size could be plotted and studied independently. An overall performance plot of power density versus flow rate with droplet size as a parameter is given in Figure 8.

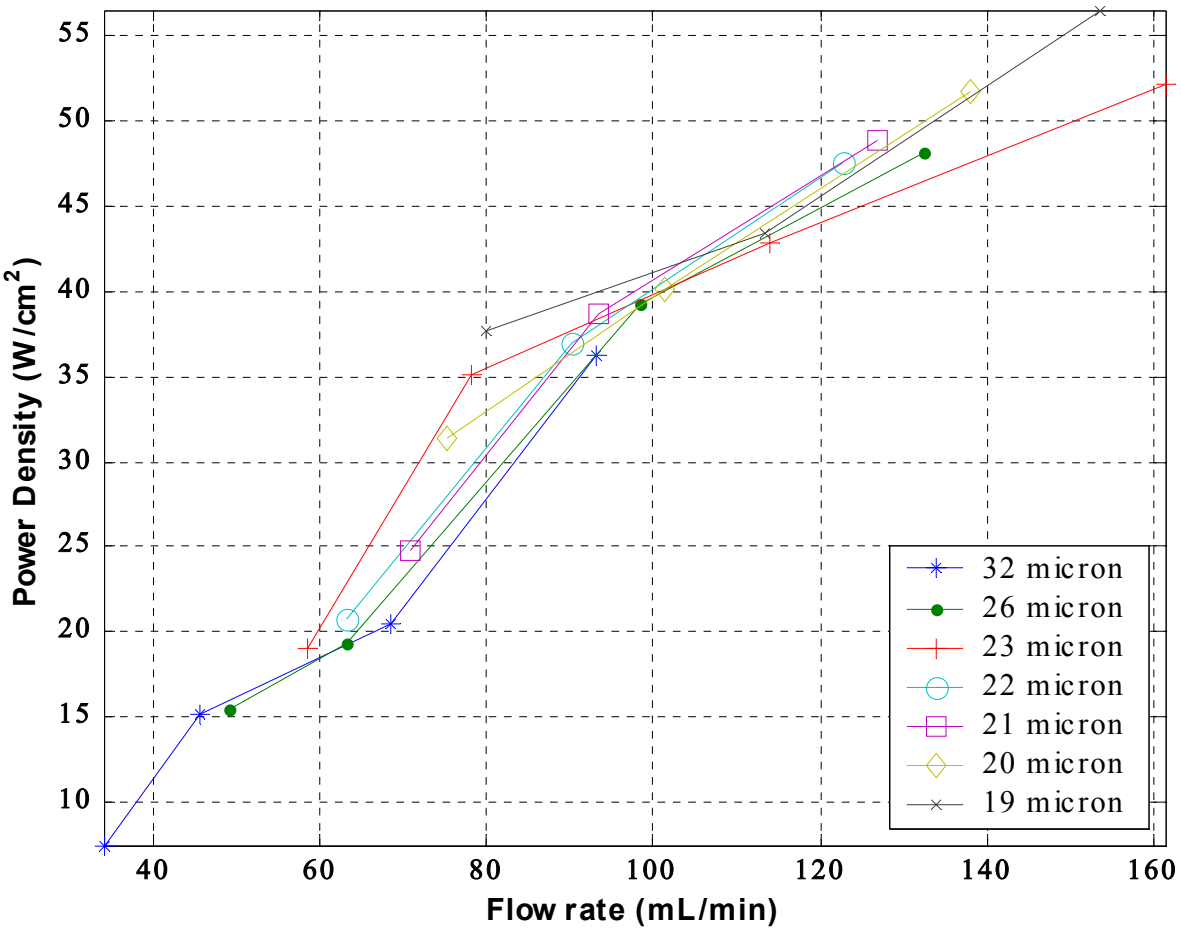

Figure 10. Heat Removal Rate for Varying Flow Rates with Droplet Size as a Parameter

A. VARIATION OF MASS FLOW RATE

The general trend regarding the heat removal capacity versus mass flow rate is easily discerned from Figure 3. In all cases, given a constant droplet size, the heat flux of the system increases with increasing mass flow rate. This result is consistent with those reported in previous works under nucleate boiling conditions (Sehmbey [1994], Halvorson [1994], Webb [1992], Yao [1987]). The observation of increasing heat flux with increasing mass flow is due to the fact that when the quantity of droplets is increased, replacement water evaporated in the liquid film surface increases. In Sehmbey [1995], spray cooling effects such as convection heat transfer, evaporation from the film surface, nucleation boiling at the heater surface, and secondary nucleation were all related to incrementing the fluid delivery rate to the surface. The secondary nucleation phenomenon was claimed to result from the entrapment of vapor bubbles by impinging liquid droplets in the liquid film. This effect is influenced by high flow in spray cooling. Bubbles from secondary nucleation can get close enough to the heat transfer surface to permit microlayer evaporation (Ortiz [1999]).

B. VARIATION OF DROPLET SIZE

The variation of heat flux removal rate with droplet size is apparent from Figure 3. It is observed that the general trend is for the heat flux to have a strong dependence on droplet size at lower flow rates ($\sim<$ 100 mL/min) and a weaker dependence at higher flow rates. These trends were also observed by Liu [2002] in his study of mist cooling. That work proposes that the heat removal capacity can be divided into two different patterns according to the mass flux of the spray flow. One is the liquid droplets drying pattern that occurs when the droplets that fall onto the heated surface are completely evaporated in the low mass flux range. The other is the liquid film fragmentation pattern that occurs when the liquid film fragments on the hot surface in the high mass flux range.

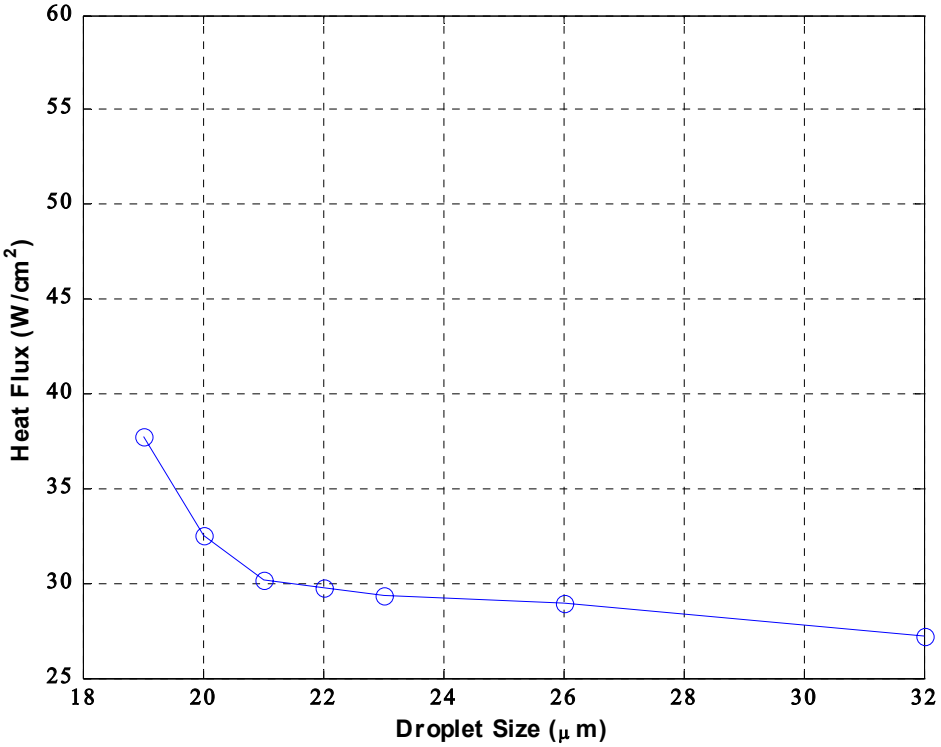

Figure 11. Behavior of Heat Flux with Droplet size at Low Mass Flow Rate (80 mL/min)

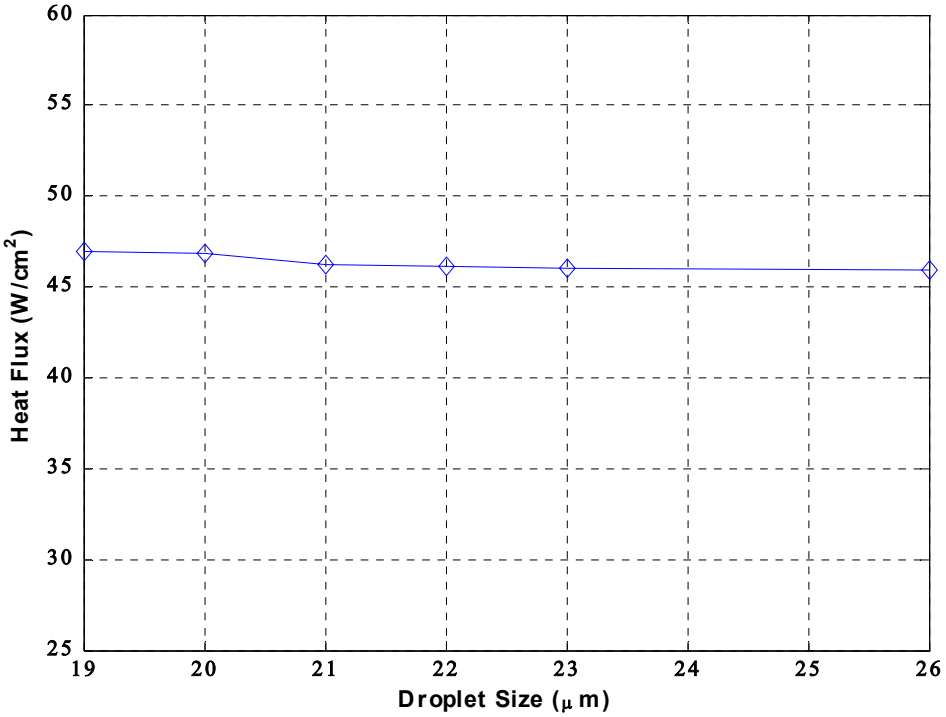

Figure 12. Behavior of Heat Flux with Droplet Size at High Mass Flow Rate (120 mL/min)

1. Low Mass Flow Range

Figure 11 illustrates the behavior of the heat flux in the low mass flow range (80 mL/min). It is observed that the heat removal capacity of the system exhibits a relatively strong dependence on the droplet size at this flow range, especially as the droplet size drops below 21 μm, the relationship being that as droplet size is decreased, the heat flux of the system increases. At low flows, the droplet size is important because for a given flow rate, a smaller mean droplet diameter gives a greater mean surface area presented by the fluid for heat transfer. This is important in the nucleate boiling region of the boiling curve to maintain a stable liquid layer that is cooled and replenished on a continuous basis by the incoming spray droplets.

The droplet size and spread are also important in the low flow range due to the film formation mechanism observed and described by Xia [2002]. Following initial contact between the droplets and the dry heated surface, the forward liquid motion was arrested by the solid surface and flow was diverted radially. As a droplet reached its maximum extent (2.2~3.0 times the initial diameter), its neighbors also reached their maximum extent and connected with each other to form a whole thin liquid film. As the film formed on the heated surface and nucleate boiling initiated, the next droplets enter the film, thereby cooling the film and replenishing any fluid lost by evaporation.

2. High Mass Flow Range

Figure 12 illustrates the behavior of the heat flux with varying droplet size in the high mass flow range (120 mL/min). It is observed that the dependence on droplet size in this range is weak to the point of being considered virtually negligible. Droplet size is less important at the higher range because the mass flux is such that the film is being cooled and replenished on a continuous basis without the reliance on droplet spreading and connection.

C. EFFECTS OF OTHER PARAMETERS

There are a variety of experiments in the literature that have examined the effects that several parameters have on the heat removal capacity of the spray system. These are divided into two categories: spray conditions and surface conditions. Spray conditions include nozzle type, mass flux, droplet size, impact velocity, and fluid subcooling. Surface conditions include roughness, level of oxidation, and impact angle. The general trends regarding these parameters are summarized as follows:

Mass Flux As mass flux is increased, heat removal capacity increases.

Droplet Size Decreasing droplet size provides better heat removal capacity for lower flow rates and has a lesser effect at higher flow rates.

Impact Velocity Impact Velocity has a negligible effect on the CHF.

Fluid Subcooling Generally, greater subcooling will have a positive effect on the CHF, although some have reported an adverse effect for very smooth surfaces (Ortiz [1999]).

Surface Roughness A "rough" surface generally provides better cooling than a "smooth" surface.

Level of Oxidation Surface oxidation has the effect of shifting the boiling curve to the right, i.e. a greater surface temperature is required to achieve the same heat flux.

Impact Angle Spray impact normal to the heated surface provides the greatest CHF performance, while decreasing angles of incidence results in lower performance.

D. PARAMETERIZATION OF THE RESULTS

1. Theoretical Considerations

It was observed in the preceding sections that the heat removal capacity of the system showed a strong dependence on the mass flux for the whole range of experimentation whereas the effect of droplet size was a secondary consideration at low flow ranges and virtually negligible at higher flow ranges. Given these observations, a new parameter was developed to take into account both the mass flow rate and the droplet size, characterizing the flow as a rate at which fluid area available for heat transfer is being added to the thin film on the heated surface.

Droplet sizes were given from the nozzle manufacturer as a Sauter mean diameter (D_{32}). Sauter mean diameter is a number used to express the average droplet size in terms of the average ratio of volume to surface area of the droplets. Since it deals with surface area, sauter mean diameter is a good way to describe a spray that is to be used for processes involving evaporation. Sauter mean diameter is the diameter of a hypothetical droplet whose ratio of volume to surface area is equal to that of the entire spray. This is expressed mathematically as

$$D_{32} = \frac{V_{droplet}}{A_{droplet}} = \frac{V_{spray}}{A_{spray}}$$

Taking this definition of the Sauter mean diameter and combining it with the relationships for the surface area and volume of the sphere, a parameter that takes into account the flow rate and the droplet size (A_{flux}, the area flux) can be developed as follows:

$$\frac{V_{droplet}}{A_{droplet}} = \frac{V_{spray}}{A_{spray}}$$

$$\text{taking } V_{spray} \text{ as the volumetric flow rate} \left(\frac{\text{cm}^3}{\text{s}}\right), \; A_{spray} \text{ now becomes } A_{flux} \left(\frac{\text{cm}^2}{\text{s}}\right)$$

$$A_{flux} = \frac{\dot{V}_{spray} * A_{spray}}{V_{droplet}} = \frac{\dot{V}_{spray}}{D_{32}}$$

2. Characterization of Heat Flux by Area Flux

Parameterizing the flow rate by the Sauter mean diameter is a convenient way of capturing the behavior of the hydraulic parameters of the fluid in one variable. A simple trend analysis on the resulting A_{flux} indicates that a larger fluid heat transfer area is available for a smaller droplet size at a given volumetric flow rate while at larger flow rates, the droplet size has less of an effect.

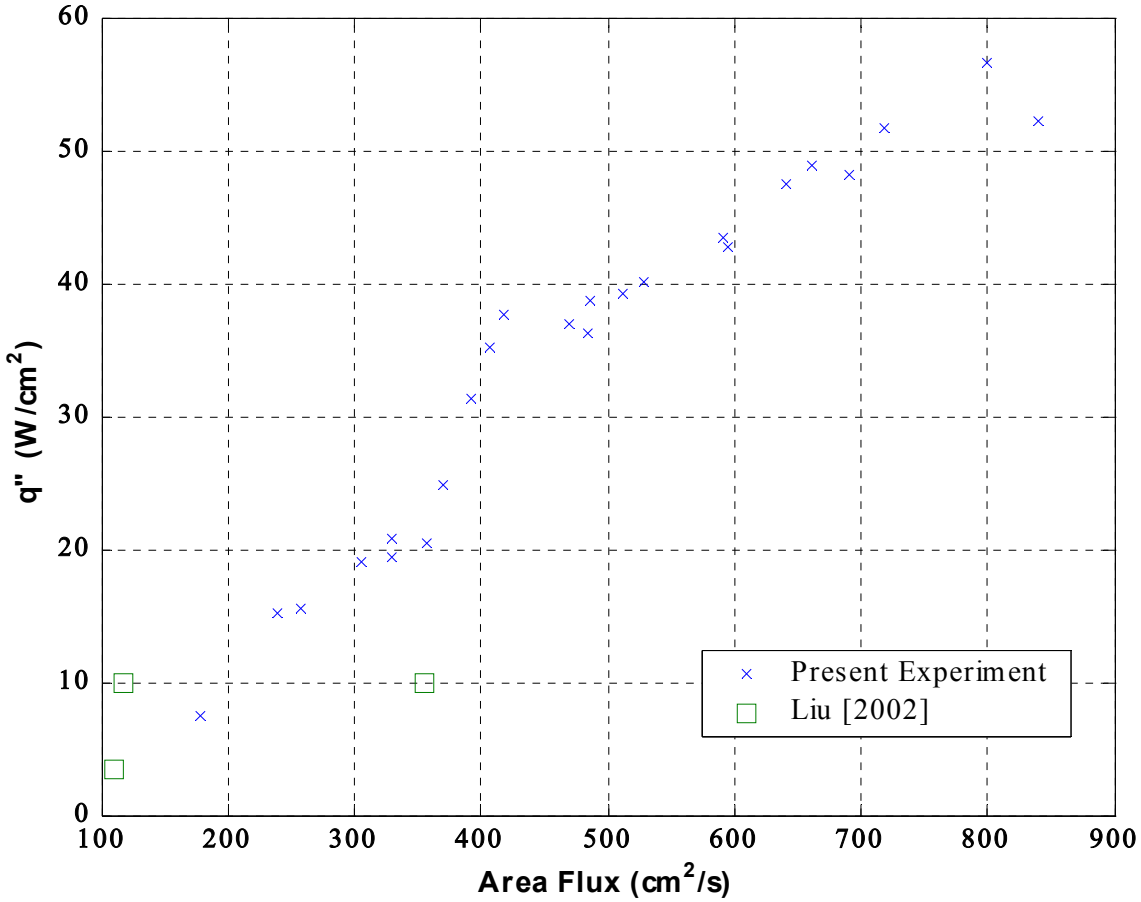

Figure 13. Power Density Plotted as a Function of the Area Flux of the Fluid and compared with a similar study

Figure 11 illustrates the results of parameterizing the flow rate by droplet size and then plotting the heat flux against the new parameter. The results of this parameterization suggest that A_{flux} is a valid way to express the effects of droplet size and flow rate in the fluid as one convenient variable. Physically, A_{flux} provides a sense for the rate at which the total surface area available for heat transfer is being replenished in the film, and when taken into account with other properties of the spray medium, it provides a sense for the overall capacity of the medium to remove heat from the surface.

3. Comparison to Previous Works

A comparison with the work conducted by Liu [2002] is provided in Figure 11 to give context to the results of the present study. This is one of the few works in the literature whose experimental parameters were similar enough to the present experiment to warrant a comparison. They studied critical heat flux under air-assisted mist cooling for flow rates of .19 to 6.35 mL/s and droplet sizes ranging from 17 to 178 μm, yielding area fluxes on the low end of the present experiment. It is observed that their data at 105 ^{o}C and the data for the present experiment are in close agreement.

There is very little data available in the literature for experiments that have focused on the nucleate boiling regime of the boiling curve for mist/spray cooling of a heated surface. The vast majority of these works have focused on obtaining a value for the critical heat flux (CHF) for a given set of experimental parameters. While CHF is an important indicator of the maximum theoretical heat removal capacity of a given system, it is dangerous to operate sensitive components at that point because of its inherent instability: a very small increase in heat flux at this point results in a very large rise in the surface temperature, which is necessary to continue to remove the heat against a suddenly very large resistance as the liquid film vaporizes. The unsteadiness of the surface temperature (and therefore its lack of controllability) at CHF was illustrated by Ortiz [1999]. The present experiment was focused on the practical operation of a spray cooling system to maintain a component at a stable temperature while taking advantage of the increased convection coefficient offered by nucleate boiling. It is within this

context that the following data in Table 4 is given to illustrate the ultimate capabilities of spray cooling under a variety of experimental conditions.

Author	Droplet Diameter	Water Temperature, C	Nozzle Type	Mass flow rate, L/h	CHF, W/cm^2
Halvorson et al [1994]	2.96-3.41 mm	20	19 gauge needle	0.07	100
Yang et al. [1993]	10-18 μm	20	Air assisted	0.5	160
Gaugler [1966]	128-150 μm	20	Full cone	0.86	240
Ortiz et al. [1999]	85-100 μm	24	Full cone	1.48-1.89	322
Kato et al. [1994]	110 μm	20	Full cone	2.04	180
Toda [1971]	88-146 μm	55-100	Air assisted	2.92	600
Xia [2002]	100-300 μm	100	Piezo-electric Silicon Block	N/A	924

Table 4. Critical Heat Fluxes achieved in previous works for various experimental conditions

It is observed that very high power densities (up to ~1 kW/cm^2) can be sustained at the CHF point and power densities greater that 100 W/cm^2 are commonly reported. The latest research is moving toward nozzle technologies (Xia [2002]) that provide extremely precise control of droplet size, flow rate, and spray pattern. Xia explored the effectiveness of an etched silicon block nozzle affixed to a pressurized chamber that was

pulsed with piezo-electric excitation. Another article reported on research into a nozzle that provided precise targeting of hot spots on the component being cooled.

E. PREDICTIVE CORRELATION

A mathematical correlation was developed to predict the behavior of the system under various spray medium hydrodynamic properties as well as the experimental parameters under the present study. This was done to assist with the modeling of future works and to gain physical insight into the response of the system.

The convection coefficient, and ultimately the power density of the system could depend on the difference between the surface and saturation temperatures, $\Delta T = \left| T_s - T_{sat} \right|$, the body force arising from the liquid-vapor density difference, $g(\rho_l - \rho_v)$, the latent heat h_{fg}, the surface tension σ, a characteristic length L, and the thermophysical properties of the fluid ρ, μ, c_p, k, the properties of the flow: mass flux Φ, droplet size D_{32}, and surface properties. The large number of interrelated variables makes it difficult to develop a theoretical correlation that is suitable for application to a wide range of experimental conditions. A number of highly empirical and ultimately extremely limited correlations exist in the literature. Therefore, the correlation developed for the present study is an attempt to capture the essence of the variety of factors that influence the heat flux, but is still semi-empirical with respect fitting the correlation to the data presented in the present work.

The first and most useful correlation for pool nucleate boiling was developed by Rohsenow [1952]

$$q''_{s,R} = \mu h_{fg} \left[\frac{g(\rho_l - \rho_v)}{\sigma} \right]^{1/2} \left(\frac{c_{p,l} \Delta T_e}{C_{s,f} h_{fg} \, \mathrm{Pr}_l^n} \right)^3$$

where the subscripts l and v denote the saturated liquid and vapor states, respectively. The bracketed term to the ½ power accounts for the buoyant body forces due to the bubble formation, and the cubic term is a dimensionless parameter that accounts for the sensible heat of a subcooled fluid. The coefficient $C_{s,f}$ and the exponent n depend on the surface-liquid combination and representative values may be obtained in the literature.

For the present experiment, the water-scored copper values were taken as $C_{s,f}$ = 0.0068 and n = 1.0. Although typical dimensionless parameters are not explicitly included, it is observed that

$$q'' \propto Ja^3 \, \mathrm{Pr}^{-3n}$$

where Jakob number $Ja = \dfrac{c_{p,l}\Delta T_e}{h_{fg}}$ is the ratio of the sensible energy absorbed by the liquid to the latent energy absorbed by the liquid during boiling. It should be noted that this correlation was developed for nucleate pool boiling of a completely wetted surface under a stagnant fluid, and for the present study is a constant. In the context of nucleate boiling heat transfer under spray cooling, the Rohsenow heat flux is seen as the power density that can be sustained by the thin fluid film under otherwise stable conditions, without taking into account hydrodynamic flow variables. While it does not account for flow variables, it does, however, provide a means for accounting for a number of fluid properties and lends itself to modification by an appropriate scaling factor to account for the hydrodynamic properties of the flow. This scaling is a measure of the enhancement in the cooling provided by the spray flow as it cools and replenishes the film. It is proposed for the present study that a function of the area flux is an appropriate scaling factor, and results in an empirical correlation for the present experiment as follows

$$q'' = q''_{s,R} * \ln(f(A_{flux}))$$
$$f(A_{flux}) = a(\frac{A_{flux}}{b})^c$$

where *a, b,* and *c* are experimentally determined curve-fit parameters. The final form of the correlation for the present study is

$$q'' = 7.36 \ln(f(A_{flux}))$$
$$f(A_{flux}) = 1.6\left(\frac{A_{flux}}{177.6}\right)^{4.56}$$

and is plotted in Figure 14 along with the experimental data to illustrate the fit. The parameters *a* and *c* are dimensionless, while *b* has the dimensions cm^2/s. The heat flux *q"* is in W/cm^2. It is observed that the correlation predicts the data within +/- 15% .

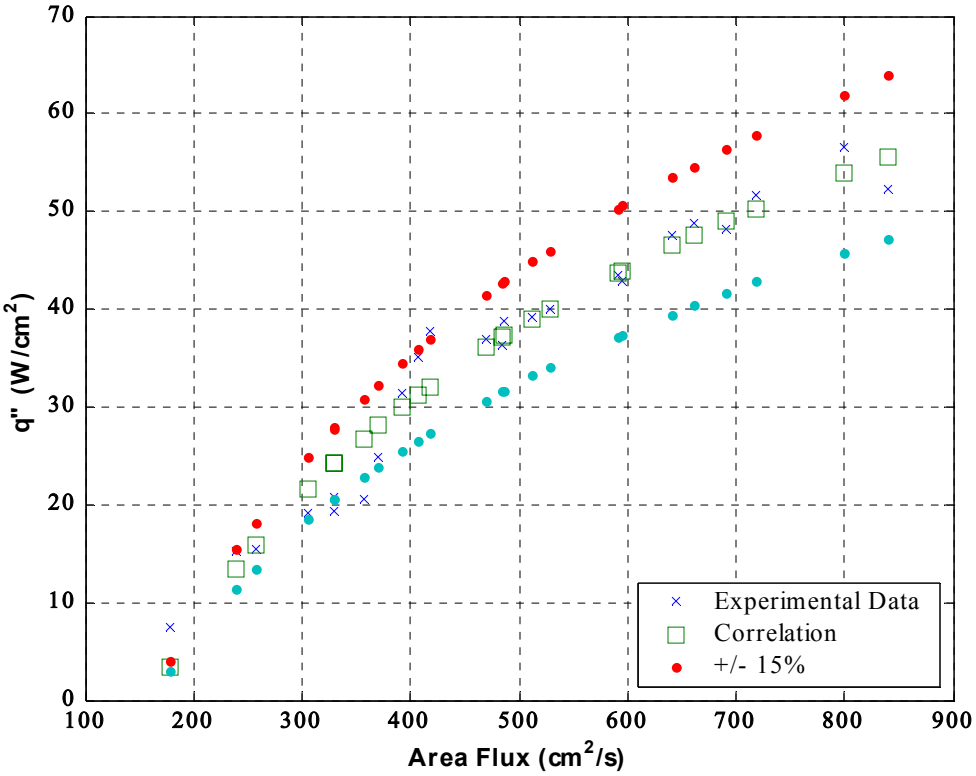

Figure 14. Comparison of Correlation with Experimental Data

V. CONCLUSIONS

An experimental study was conducted to investigate the validity of using spray cooling to remove high heat fluxes resultant from high power density generation from microelectronic devices. The effects of mass flow rate and droplet size were studied independently and the results indicate the following:

1. The heat flux is strongly dependent on the mass flow rate of the spray in all regimes of flow.
2. The heat flux depends secondarily on the droplet size of the fluid at low mass flows and very weakly on the droplet size at greater flows.
3. The hydrodynamic characteristics of the spray flow can be combined into one parameter, the area flux, and the heat flux can be correlated to this parameter.
4. The results show that spray cooling in the nucleate boiling regime offers significant heat removal capacity that can be improved upon with further work.

A semi-empirical correlation was developed to provide a framework for modeling future works and to gain physical insight to the present work. Its empirical nature suggests the need for further work to provide better resolution and to test its applicability in other regimes.

Further work is necessary to elucidate and/or validate the results of the present experiment, including the study of a wider range of flow rates and droplet sizes to improve/validate the correlation, boiling at higher surface temperatures, boiling at partial vacuum to provide lower saturation and therefore lower surface temperatures, and the investigation of novel nozzle technologies.

THIS PAGE INTENTIONALLY LEFT BLANK

VI. LIST OF REFERENCES

B.W. Webb, M Queiroz, K. N. Oliphant, and M. P. Bonin, Onset of Dry-Wall Heat Transfer in Low-Mass-Flux Spray Cooling, *J. Exp. Heat Transfer,* vol. 5, pp. 33-50, 1992.

C. Xia, Spray/Jet Cooling for Heat Flux High to 1 kW/cm^2, *18th IEEE SEMI-THERM Symposium,* pp. 159-163, 2002.

D. Kearns, J. Du, R. H. Chen, and L. C. Chow, A Parametric Study of Dielectric Spray Cooling of a Row of Heaters in a Narrow Channel, *18th IEEE SEMI-THERM Symposium,* pp.164-168, 2002.

F. K. McGinnis and J. P. Holman, Individual Droplet Heat-Transfer Rates for Splattering on Hot Surfaces, *Int. J. Heat Mass Transfer,* vol. 12, pp. 95-108, 1969.

J. D. Bernardin, C. J. Stebbins, and I. Mudawar, Effects of Surface Roughness on Water Droplet Impact History and Heat Transfer Regime, *Int. Journal Heat Mass Transfer,* vol. 40, pp. 73-88, 1997.

J. I. Gonzalez and L. Ortiz, Experiments on Steady-State High Heat Fluxes Using Spray Cooling, *Experimental Heat Transfer*, vol. 12, pp. 215-233, 1999.

J. Yang, M. R. Pais, and L. C. Chow, Critical Heat-Flux Limits in Secondary Gas Atomized Liquid Spray Cooling, *J. Exp. Heat Transfer,* vol. 6, pp. 55-67, 1993.

M. Kato, Y. Abe, Y. H. Mori, and A. Nagashima, Spray Cooling Characteristics under Reduced Gravity, *J. Thermophysics,* vol. 9, pp. 378-381, 1994.

M. R. Pais, L. C. Chow, and E. T. Mahefkey, Surface Roughness and Its Effects on the Heat Transfer Mechanism in Spray Cooling, *J. Heat Transfer,* vol. 114, pp. 211-219, 1992.

M. S. Sehmbey, L. C. Chow, M. R. Pais, and T. Mahefkey, High Heat Flux Spray Cooling: A Review, *Proc. ASME Heat Transfer Div.,* vol. 301, pp. 39-45, 1994.

M. S. Sehmbey, L. C. Chow, O. J. Hahn, and M. R. Pais, Effect of Spray Characteristics on Spray Cooling with Liquid Nitrogen, *J. Thermophys. Heat Transfer,* vol. 9, pp. 757-765, 1995.

P. J. Halvorson, R. J. Carson, S. M. Jeter, and S. I. Abdel-Khalik, Critical Heat Flux Limits for a Heated Surface Impacted by a Stream of Liquid Droplets, *J. Heat Transfer,* vol. 116, pp. 679-685, 1994.

R. E. Gaugler, An Experimental Study of Spray Cooling of High Temperature Surfaces, Ph. D. thesis, Carnegie Institute of Technology, Pittsburgh, 1966.

S. C. Yao and K. J. Choi, Heat Transfer Experiments of Mono-Dispersed Vertically Impacting Sprays, *Int. J. Multiphase Flow,* vol. 13, pp. 639-648, 1987.

S. Toda, A Study of Mist Cooling (1st Report: Investigation of Mist Cooling), *Heat Transfer-Jpn. Res.*,vol 1, pp.39-50, 1971.

W. M. Rohnesow, A Method of Correlating Heat Transfer Data for Surface Boiling Liquids, *Trans. ASME,* vol. 74, pg. 969, 1952.

Y. M. Qiao and S. Chandra, Boiling of Droplets on a Hot Surface in Low Gravity, *Int. J. Heat Mass Transfer,* vol. 39, pp. 1379-1393, 1996.

Z. Liu, Experimental Study of the Boiling Critical Heat Flux of Mist Cooling, *Exp. Heat Transfer,* vol. 15, pp. 229-243, 2002.

VII. APPENDIX A-FLUID AND TEST SECTION PROPERTIES

$g = 9.8$ m/s^2

Fluid Properties of distilled water

$\rho_l = 957.85$ kg/m^3

$\rho_v = 595.59$ kg/m^3

$\mu_l = 279 * 10^{-6}$ N-s/m^2

$h_{fg} = 2257$ kJ/kg

$\sigma = 58.9 * 10^{-3}$ N/m

$c_{pl} = 4.217$ kJ/kg-K

$Pr_l = 1.76$

Properties of Pure Copper

$k = 392.9$ W/m-K

THIS PAGE INTENTIONALLY LEFT BLANK

VIII. APPENDIX B-SAMPLE CALCULATIONS

A. HEAT FLUX FOR B37 AT 100 PSI

The heat flux calculated using *Fourier's Law* assuming one-dimensional conduction in the axial direction. T_1, T_2, and T_3 are the heater block lower, middle, and upper temperatures, respectively, and Δx is the separation between each thermocouple. Conductivity k is the assumed value for pure copper given in appendix A.

$$q'' = k\frac{\Delta T}{\Delta x}$$

$$\Delta T = \frac{(T_1 - T_2) + (T_2 - T_3)}{2} = \frac{(120.909 - 120.282) + (120.282 - 119.693)}{2} = 0.608$$

$$q'' = 392.9 * \frac{0.608}{0.003175} = 7.52 \text{ W/cm}^2$$

B. CALCULATION OF THE ROHSENOW SURFACE HEAT FLUX

The Rohsenow surface heat flux for nucleate boiling was calculated by the following equation

$$q''_{s,R} = \mu h_{fg}\left[\frac{g(\rho_l - \rho_v)}{\sigma}\right]^{1/2}\left(\frac{c_{p,l}\Delta T_e}{C_{s,f} h_{fg} \text{Pr}_l^n}\right)^3$$

using values of all the parameters as given in Appendix A.

THIS PAGE INTENTIONALLY LEFT BLANK

IX. APPENDIX C-EQUIPMENT SPECIFICATIONS

A. NOZZLES

Manufacturer: Hago Precision Nozzles

Model Numbers: B37, B50, B75, B100

Flow Characteristics:

Model Number	100 psi	200 psi	300 psi	500 psi
B37	0.59 / 32.1	0.83 / 26.5	1.01 / 23.1	1.31 / 19.5
B50	0.79 / 33.3	1.12 / 27.6	1.37 / 23.8	1.77 / 20.5
B75	1.19 / 32.5	1.68 / 26.5	2.05 / 23.9	2.65 / 19.9
B100	1.58 / 31.3	2.24 / 27.0	2.74 / 23.2	3.54 / 19.7

Table 5. Manufacturer Provided Flow Rates/Droplet Sizes at various operating pressures (Gallons per Hour/microns)

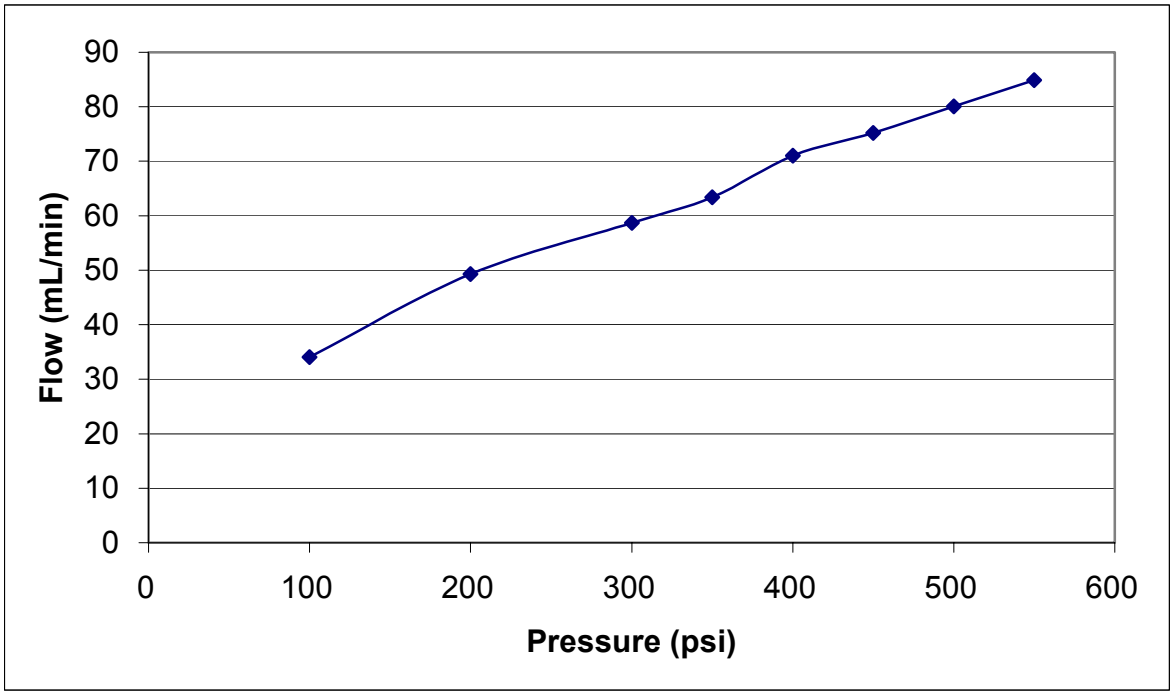

Figure 15. Typical Flow Versus Pressure Calibration Curve (Nozzle B37)

B. PRESSURE GAGE

Model: Omega DPG500-1K-D2

Range: 0-1000 psi

Output: Digital Display, 0-5 VDC analog output to data acquisition

Calibration: 0.25% FS (+/- 2.5 psi)

Voltage-Pressure Output Characteristics:

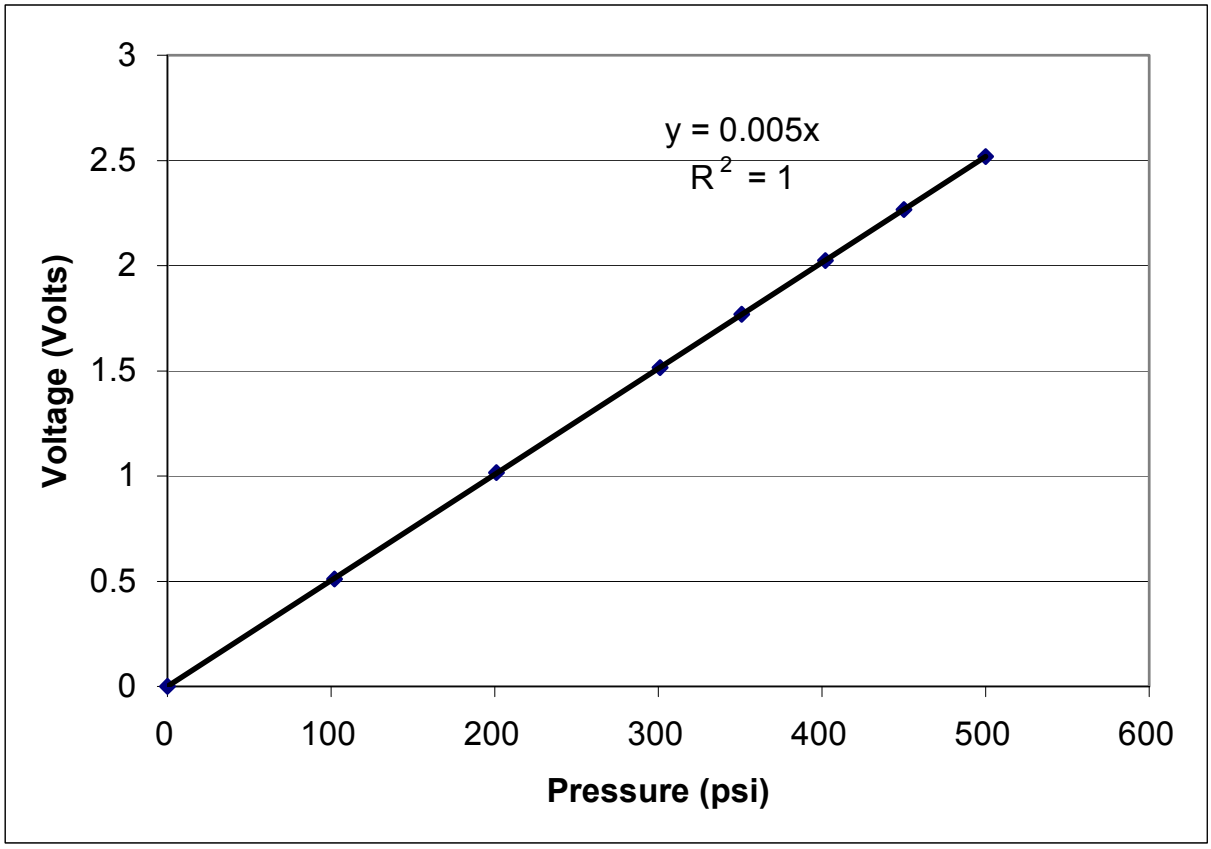

Figure 16. Voltage vs. Pressure Output Characteristics of Digital Gage

C. THERMAL EPOXY

Model: Omega OB-200 Epoxy Adhesive

Thermal Conductivity: 1.26 W/m-K

Tensile Shear Strength: 190 kg/cm^2 at 24 C, 148 kg/cm^2 at 149 C

Coefficient of Thermal Expansion: 38*10^{-6} in/in/C

Maximum Continuous Temperature: 260 C

D. THERMAL COMPOUND BETWEEN HEATER BLOCK AND TEST SECTION

Manufacturer: Antec

Model: Reference Silver Thermal Compound

Thermal Conductivity: >9.0 W/m-K

Thermal Resistance: <0.0024 C-in^2/W

Temperature Limits: -40 C to >180 C

E. VARIABLE VOLTAGE TRANSFORMER

Manufacturer: Staco

Model: 5021 CT, closed case

Input voltage: 200 Volts RMS / 60 Hz AC (building service)

Output voltage: 0-237 Volts

Maximum Current: 28 Amps

F. HEATERS

Manufacturer: Watlow

Model: J3A79-L12

Length: 3 in., Diameter: 0.496 +/- 0.005 in.

Capacity: 1000 W nominal at 120 Volts

Resistance: 14 Ohms, nominal

G. THERMOCOUPLES

Manufacturer: Omega

Model: Type E, 5SRTC-KK-E-30-36

Bead Diameter: 0.010 in.

X. APPENDIX D-DATA ACQUISITION SCHEMATIC

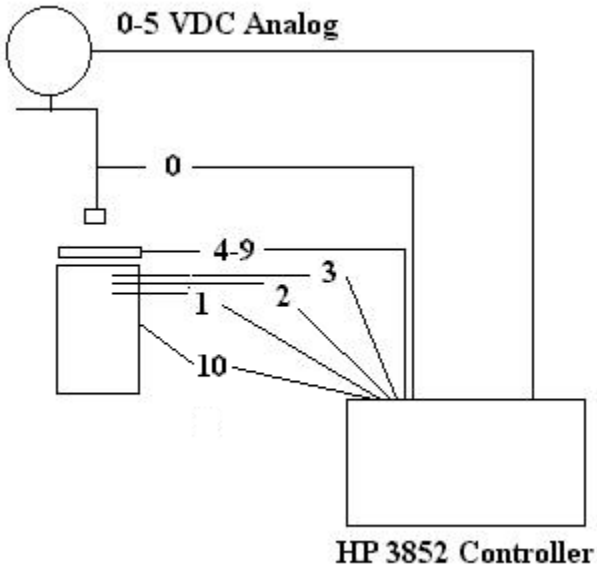

Figure 17. Data Acquisition Detail Schematic

A. THERMOCOUPLE CHANNELS

0: Fluid Temperature

1: Heater Block Lower

2: Heater Block Middle

3: Heater Block Upper

4-9: Radially across test section, surface temperatures

10: Heater Block Side

11 (not shown): PVC enclosure inner diameter

Pressure Gage output was 0-5 VDC analog

THIS PAGE INTENTIONALLY LEFT BLANK

INITIAL DISTRIBUTION LIST

1. Defense Technical Information Center
   Ft. Belvoir, Virginia

2. Dudley Knox Library
   Naval Postgraduate School
   Monterey, California

3. Professor Ashok Gopinath
   Naval Postgraduate School
   Monterey, California

4. Matthew A Cryer
   Naval Postgraduate School
   Monterey, California
5. Brad Filius
   Naval Postgraduate School
   Monterey, California

6. Young W. Kwon
   Naval Postgraduate School
   Monterey, California